SEDIMENT TRANSPORT IN RESPONSE TO WAVE GROUPS GENERATED BY HIGH-SPEED VESSELS

Philip D. Osborne[1], Neil J. MacDonald[2], and Shaun Parkinson[3]

1. Pacific International Engineering, PLLC, 123 Second Ave. South, P.O. Box 1599, Edmonds, WA, 98020, USA. philo@piengr.com
2. Pacific International Engineering, Corp, 260 Centrum Blvd., Ste 220, Ottawa, Ontario, Canada, K1E 3P4 neilm@piengr.com
3. Idaho Power Company, P.O. Box 70, Boise, ID, 83707, USA, sparkinson@idahopower.com

Abstract: Suspended sediment transport dynamics occurring at relatively short time scales under super-critical wave groups created by moving high speed vessels are investigated by means of field measurements and the application of numerical models. Examples are provided from a variety of different environments, including predominately sandy beaches in low energy estuarine and fluvial settings. Model simulations combining the hydrodynamics of the wakes with steady currents and a sand transport model provide results that are largely consistent with field measurements and observations of the suspended load fraction. Wakes re-suspend sand in the nearshore that would otherwise be immobile and move it incrementally offshore and alongshore, eventually into deeper water where stronger ambient flows (tidal or fluvial) can transport the sediment. Super-critical wakes from high speed vessels have a tendency to cause offshore transport of sand-sized sediment leading to beach flattening while their sub-critical counterparts often lead to beach steepening.

INTRODUCTION

Wave-induced erosion associated with ship traffic in confined waterways has been widely reported including locations in San Francisco Bay, California, Puget Sound, Washington, Georgia Strait, British Columbia, Saint Lawrence River, Quebec, Waitemata Harbor and Marlborough Sounds, New Zealand, Loch Ryan, Scotland and Kattegatt, Denmark (see review by Parnell and Kofoed-Hansen, 2001). Because of their size and speed, many commercial and recreational vessels are capable of producing sizable wakes that can be damaging to the adjacent shoreline and dangerous to other craft. Unfortunately, there is little design information and few unified design tools are available to scientists and engineers needing to predict the sediment transport and associated morphological effects on shorelines resulting from vessel wakes. This paper examines the details of the fluid and suspended sand dynamics that occur at medium (hours) and short (seconds) time scales on beaches with a range of grain sizes (sand-pebble) present in response to super-critical wave groups created by moving high speed vessels. Examples are provided from Snake River, Idaho and Auckland, NZ. The purpose is to gain insight into the differing modes of transport for coarse- and fine-grained sediments under wakes produced by high speed vessels.

SUPER-CRITICAL AND SUB-CRITICAL WAKES

A vessel wake observed at the shoreline in a coastal, estuarine, or fluvial environment occurs as a sequence or group of waves. The characteristics of the wave group observed at the shoreline depend on a large number of variables related to the moving vessel including position, heading, and distance from shore, speed, hull geometry, trim and displacement, as well as the properties of the ambient water body including depth contours, presence of currents, or wind waves. The term *super-critical* is sometimes used to describe high-speed vessels while the term *sub-critical* is used to describe displacement vessels traveling at slow speed. Super-critical refers to the state where the vessel is moving faster than the speed at which a wave of the same length can travel in that depth of water. The super-critical condition depends on the speed of the vessel and the depth of the water. The wake produced by a super-critical vessel is different from that produced by a vessel moving at sub-critical speed (see Osborne et al., 2006 for examples). In the latter case, the wake produced has both diverging and transverse components. The transverse component is monochromatic and its wavelength is determined from the linkage between the speed of the vessel and the celerity of the wake for the given depth of water. Whereas the spectrum of a super-critical wake shows peaks in energy at a number of frequencies and the wake passing a point shows a steady decline in wave period through time.

Figure 1a illustrates the classical wake pattern generated by a sub-critical vessel. The wake is composed of two types of waves; diverging wakes that move away from the vessel at an angle of 35.27^{o} and transverse wakes that move in the vessel's direction. Both types of wakes theoretically exist only within a cone set at 19.47^{o} from the vessel. This pattern, first described mathematically by Lord Kelvin in 1887, can be derived from simple geometry. The wavelength and speed of the wake can be found from linear wave theory. As the vessel speed increases, so does the celerity of the wake. A point will be reached where the vessel is moving faster than its transverse wake and this part of the wake is shed. From this point on (i.e. if the vessel maintains a speed equal to or greater than this speed and the depth remains the same or decreases) the wake will assume a new form; the super-critical wake pattern is composed only of diverging wakes (Figure 1b). The super-critical wakes cannot exist as free gravity waves in a classical Kelvin wake pattern. Super-critical vessels produce a wake pattern in which the period of the waves appears, to a stationary observer, to decrease in an approximately exponential manner.

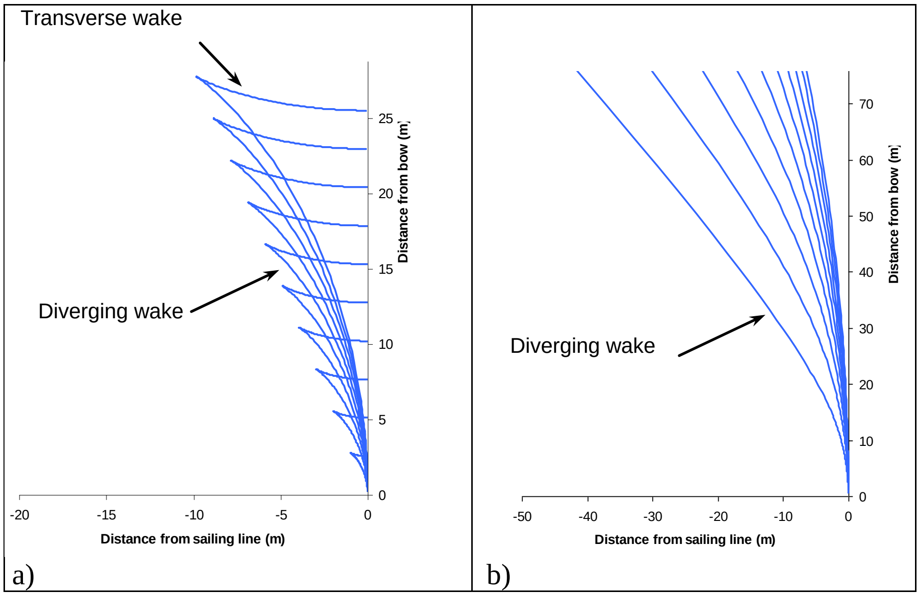

Figure 1. Wake patterns: a) sub-critical vessel; and b) super-critical vessel

METHODS

The approach in this paper involves a combination of detailed and direct field measurements and numerical modeling of the relevant processes. Field measurements were obtained from three different environments:

- a mixed sand and gravel beach exposed to wind waves, wakes from both conventional and high speed commercial and recreational vessels, and strong tidal currents in Puget Sound, Washington (see Osborne et al., in press),
- sand and gravel bars exposed to wakes from jetboats and river flows in the Hells Canyon Reach of Snake River, Idaho and
- a sandy foreshore exposed to wakes and wind waves in the Waitemata Harbor Auckland, NZ.

The approach to modeling is demonstrated with examples from a sand bar in the Snake River, Idaho.

Field Measurements

Field measurements collected and analyzed for this paper include time series of wakes and water surface elevations measured with pressure sensors or capacitance wires, 3D orbital velocities measured with Acoustic Doppler Velocimeter (ADV), and suspended sand concentrations (*ssc*) measured with Optical Backscatter Sensors (OBS). The ADV was integrated with other sensors as part a Sontek HYDRA system (Figure 2).

The sediment dynamic response under wakes and ambient conditions was determined by direct visual observation of sediment motion and recording of *ssc* time series with OBS. Calibration of the OBS to determine *ssc* was achieved using local sediment in a laboratory calibration facility following typical procedures for sandy sediments.

Wakes from a variety of different high speed vessels including recreational jet boats, conventional catamarans, and foil-assisted catamarans are considered. Measured wake time series were analyzed to compute wake wave characteristics using zero-crossing analysis and spectral analysis methods. The measurements allow validation of numerical models, but also provide valuable insights on processes occurring under boat wakes that lead to improvements in modeling.

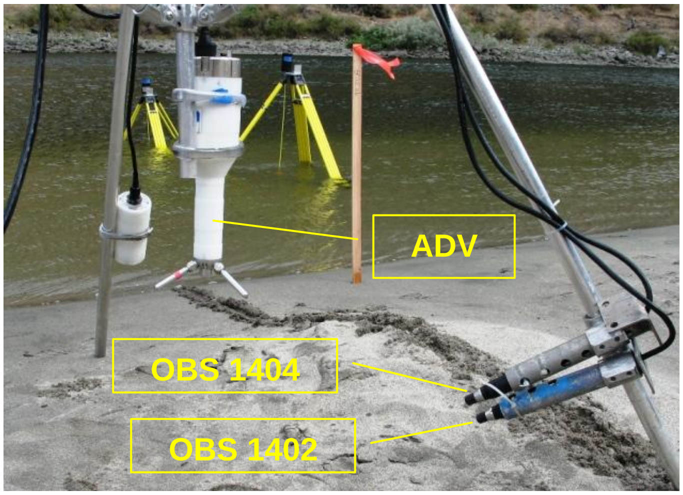

Figure 2. Sontek HYDRA system consisting of ADV and 2 OBS

Numerical modeling

Computer model application in the study includes tidal and river circulation models, wind wave models, a new wake prediction model for high speed vessels, and a Lagrangian sediment transport model. The approach to modeling is demonstrated in this paper with an example from the Fish Trap sand bar in the Snake River, Idaho. The general approach of the modeling exercise is as follows:

- Computer modeling with the Lagrangian Super critical Vessel (LSV) model, an enhanced 2D wake prediction model (MacDonald, 2005), is used to predict the spatially- and temporally-varying wake train produced by a powerboat as it passes a sand bar.
- The wake data is combined with flow data from a large-scale hydrodynamic model (MIKE 21C, IPC) of the river to predict the potential sediment transport caused by this single boat passage (i.e. the sediment put into suspension).
- A medium-term particle tracking simulation (48 hours) is performed with a Lagrangian Particle Tracking Model (PTM, MacDonald et al., 2006) to determine the transport of this sediment. This stage is performed with and without subsequent boat passes. PTM is used to simulate the pattern and magnitude of net sediment transport on the sand bars under the combined influence of boat wakes and river flows.
- An assessment of the fate (i.e. the percentage of material no longer in the vicinity of the sand bar) is made for both the river-only and river plus

powerboat simulations to identify the impact of boating on the movement of sediment at the sand bar.

The preceding bullets identify an approach for the quantitative determination of the impact of boating on a select mass of sediments – those put into suspension by the first boat passage in the 48 hour period. The purpose of the modeling is to develop quantitative estimates of the relative role of boat wakes and river flows in causing mobilization of sediment on sand bars with the possibility of developing preliminary estimates of the potential for net transport from the bars. The approach does not consider the fate of any new sediment put into suspension by subsequent wake events, but there is no reason to believe that these new sediments would behave in a different manner. As well, the approach does not consider delivery of fine sediments to the sand bar by the river during high-flow events.

To better account for wave action, especially wave breaking in the nearshore, a new potential sediment transport equation developed by Camenen and Larsen (in press) was added to PTM. The Camenen and Larsen formula is a total load (i.e. bed load and suspended load) potential transport formula. The total transport rate is given by:

$$q_t = \frac{u_* a}{g(\rho_s - \rho)} \frac{\tau_{cw}}{\left(1 + \tan\beta / \tan\Phi_m\right)} \exp\left(-b\frac{\tau_{cr}}{\tau_{cw}}\right)\left[1 + K_T \frac{h}{d_{50}} \frac{U_c}{u_* w} \sqrt[3]{D_t / \rho}\right]$$

where q_t is the volumetric, depth-integrated sediment transport rate [units of m^2/s], θ_{cr} is the critical Shields parameter, w is the sediment fall velocity, τ_c is the current-induced shear stress, τ_{wc} is the combined wave-current shear stress, ρ is the fluid density, ρ_s is the sediment density, g is gravitational acceleration, β is the bed slope, Φ_m is the moving friction angle (≈30°), D_t is the total energy dissipation, d_{50} is the median grain size, U_c is the current speed, $u_* = \sqrt{\tau_c / \rho}$ and:

$$K_T = \frac{2\gamma_o c_B k_d}{a\pi\theta_{cr}}$$

The coefficients in the above equations are a =12, b =4.5, c_B =0.65 and γ_o =2×10^{-5}.

RESULTS

Offshore mean flow during super-critical wakes

Analysis of a large number of velocity records from several locations reveals that as well as introducing an oscillatory component to the nearshore current, the super-critical boat wakes also modify the local steady current by producing an offshore-directed flow. Figure 3 shows a plot of time-averaged nearshore east and north velocity components, V_E and V_N respectively, measured during wake and no-wake intervals at Fish Trap Bar on the Snake River. The shoreline in this case runs approximately north-south and is on the west river bank; therefore positive V_E indicates an offshore directed flow. In general, the mean flows during the wakes are more easterly and larger than during the no-wake intervals. This pattern of enhanced offshore flow was consistent at all locations.

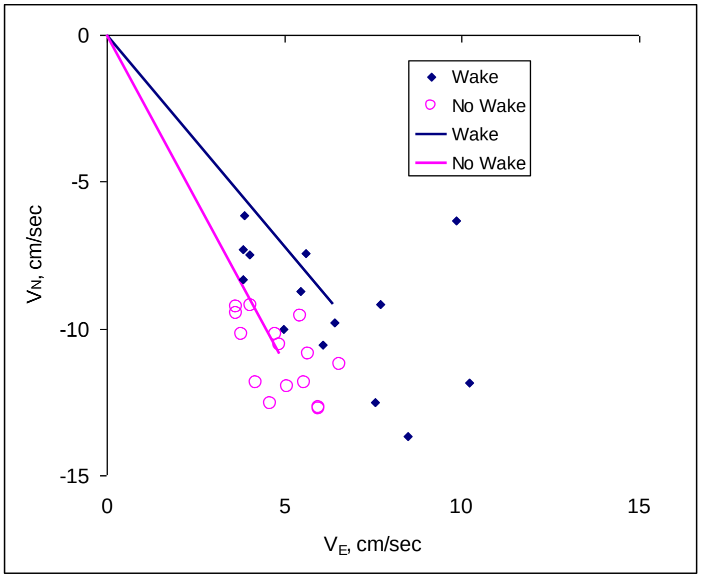

Figure 3. Time-averaged nearshore velocity components (V_E, V_N) measured during wake and no-wake intervals at Fish Trap Bar on the Snake River

The offshore-directed flow has not been previously documented in the context of vessel wakes though it appears to be analogous to a group-forced second-order flow and set-up driven undertow (e.g. Longuet-Higgins and Stewart, 1962, 1964; Doering, 1988). Figure 4 shows a time series of instantaneous near bed wave normal velocity, V_x, measured during a boat wake at Fish Trap Bar. Also shown in Figure 4 is the time variation of the velocities averaged over two to three wave periods (10 sec), $V_{x\text{-}Avg}$. A relatively simple undertow model Grasmeijer and Ruessink (2003) was found to be in good agreement with the measured flows.

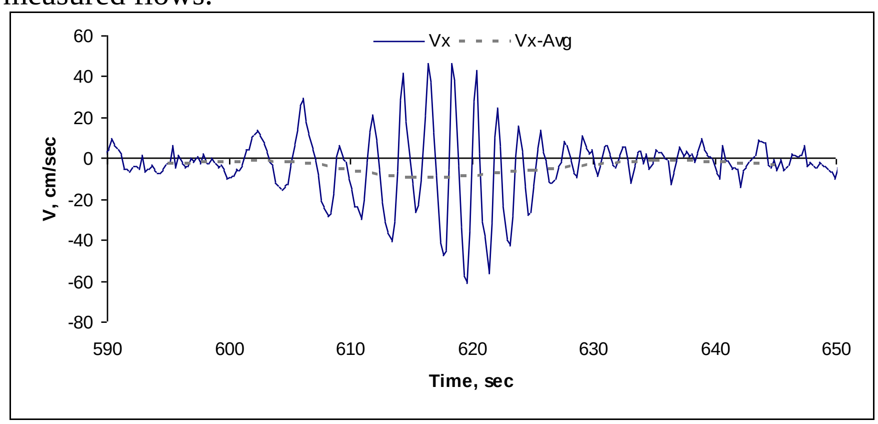

Figure 4. Instantaneous V_x under a wake and 10-sec average velocity, $V_{x\text{-}avg}$, measured at Fish Trap Bar, Snake River

Suspension of sand by super-critical wakes

Figure 5 provides examples of time series of V_x and *ssc* measured during the passage of super-critical wakes produced by different vessels over a variety of different substrates. The relevant conditions are summarized in Table 1. The V_x velocities were determined by rotation of the V_N and V_E velocities such that V_x is the principle component of flow and V_x is positive under the wave crests (approximately onshore in each case); V_y is the secondary flow and is orthogonal to V_x. Peak to peak velocities of +/- 0.40-1.0 m/sec occur under the largest waves in the wakes. The wakes produced by QuickCat result in maximum velocities which are approximately a factor of two larger than those observed in Snake River and correspondingly larger *ssc*. The wave-induced velocities in the wake train are distinctly asymmetric (nonlinear) with short, sharp-peaks under the crests and broader flatter troughs. The high velocities under the wave crests produce the largest peaks in *ssc*. The peaks in *ssc* are relatively low under the long period waves during the first half of the wake, whereas, large peaks in *ssc* occur during the higher, shorter-period waves in the middle of the wake. In most cases *ssc* remains elevated for several waves following the peak velocities.

Table 1. Summary of vessel operating conditions for selected super-critical wakes

Location	***Vessel Name***	***Date***	***TPass***	***Speed (knots)***	***Fr (depth)***	***Fr (length)***	***Distance (m)***	***Boat Length (m)***
Torpedo Bay, Auckland	*QuickCat*	1995-08-02	12:10	26	1.10	0.77	~1 km	33.4
Tin Shed, Snake River	*Hells Canyon Dream*	2005-08-27	11:59	24.5	2.32	1.10	86.0	13.41
Salt Creek, Snake River	*Happy Hour*	2005-08-28	15:50	33.2	1.82	1.65	106.0	10.97

To illustrate the relationships between wave forcing and near-bed sediment suspension on a wave-by-wave basis, phase diagrams of wave-averaged *ssc* as a function of wave-by-wave estimates of the skin friction Shields parameter (θ'_w) are shown in Figure 6 for each of the consecutive waves in the wake trains shown in Figure 5. Waves were identified by zero up-crossing analysis of time-series of V_x. Wave-by-wave estimates of θ'_w are based on U_{sig} (the average of the highest 1/3 velocity measurements under the crest of the wave), and the median sediment diameter representative of the local sediments. Measured *ssc* was averaged through each wave period.

A distinct counter-clockwise hysteresis is apparent in the phase diagrams (Figure 6). All of the phase diagrams exhibit a region of low and steady *ssc* through the first several waves while θ'_w increases well above the threshold for motion and for suspension. As θ'_w approaches a maximum under the largest waves in the wake train, *ssc* increases rapidly. The maximum *ssc* is reached during the wave following the maximum θ'_w and then begins to decline. Despite a decline in both *ssc* and θ'_w following the maximum *ssc*, the *ssc* is significantly higher while θ'_w is decreasing after the peak than that measured under waves with similar values of θ'_w during the increase before the peak. The pattern is more pronounced at higher elevations above the bed (compare green line with blue line in Figure 6 b,c) indicating a significant temporal phase lag in *ssc* with elevation.

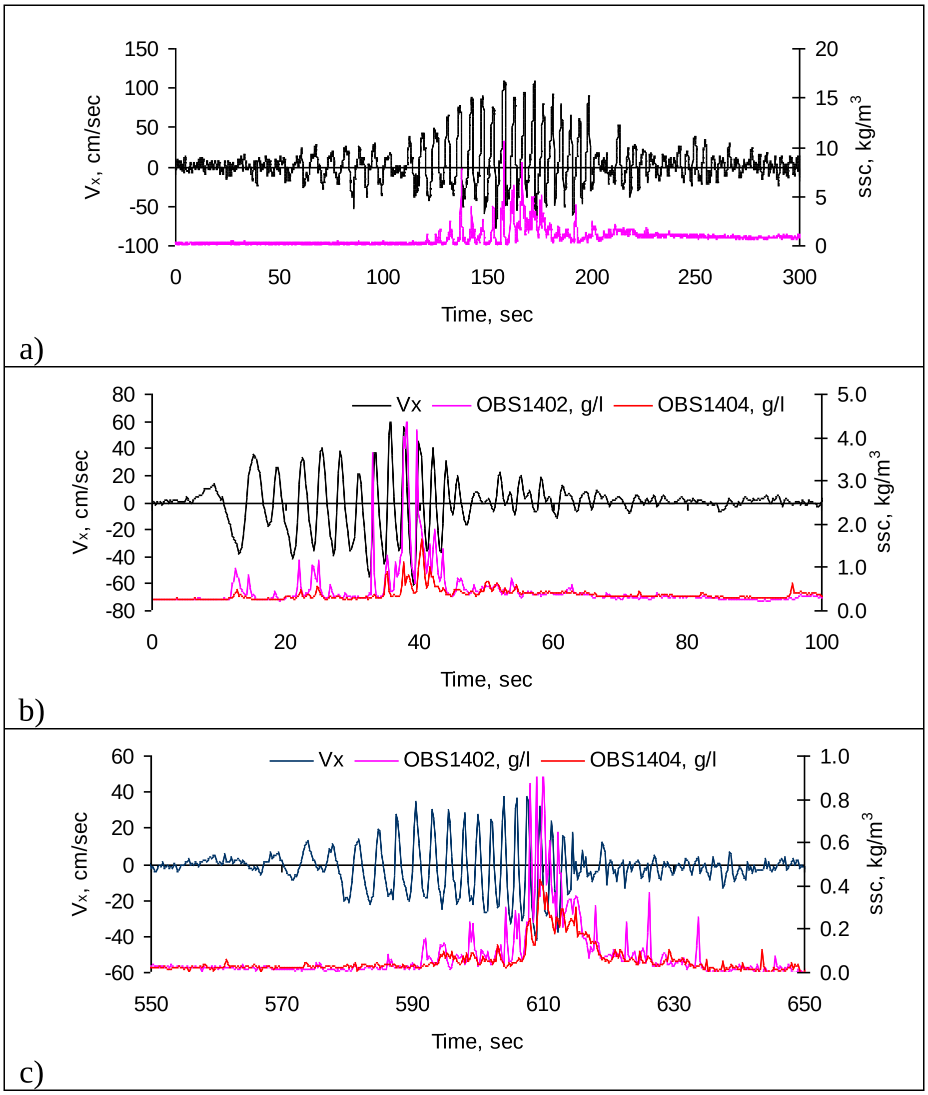

Figure 5. Time series of nearshore V_x and *ssc* under high speed super-critical wakes: a) Torpedo Bay, Auckland, *QuickCat*; b) Tin Shed Bar, Snake River, *Hells Canyon Dream*; c) Salt Creek Bar, Snake River, *Happy Hour*

Simulation of sediment transport by combined wakes and currents

The sediment modeling methodology used in the present work consists of a multi-stage approach:

- development of a detailed daily wake climate using the LSV wake model;
- development of a 48-hour flow hydrograph using MIKE 21C data;

- application of the PTM model to predict the sediment put into suspension on a typical boat passage;
- application of the PTM model to predict the transport of the sediment for a 48-hour period, and;
- analysis of the sediment fate to determine percentage retention/loss of sediment caused by the boat wakes.

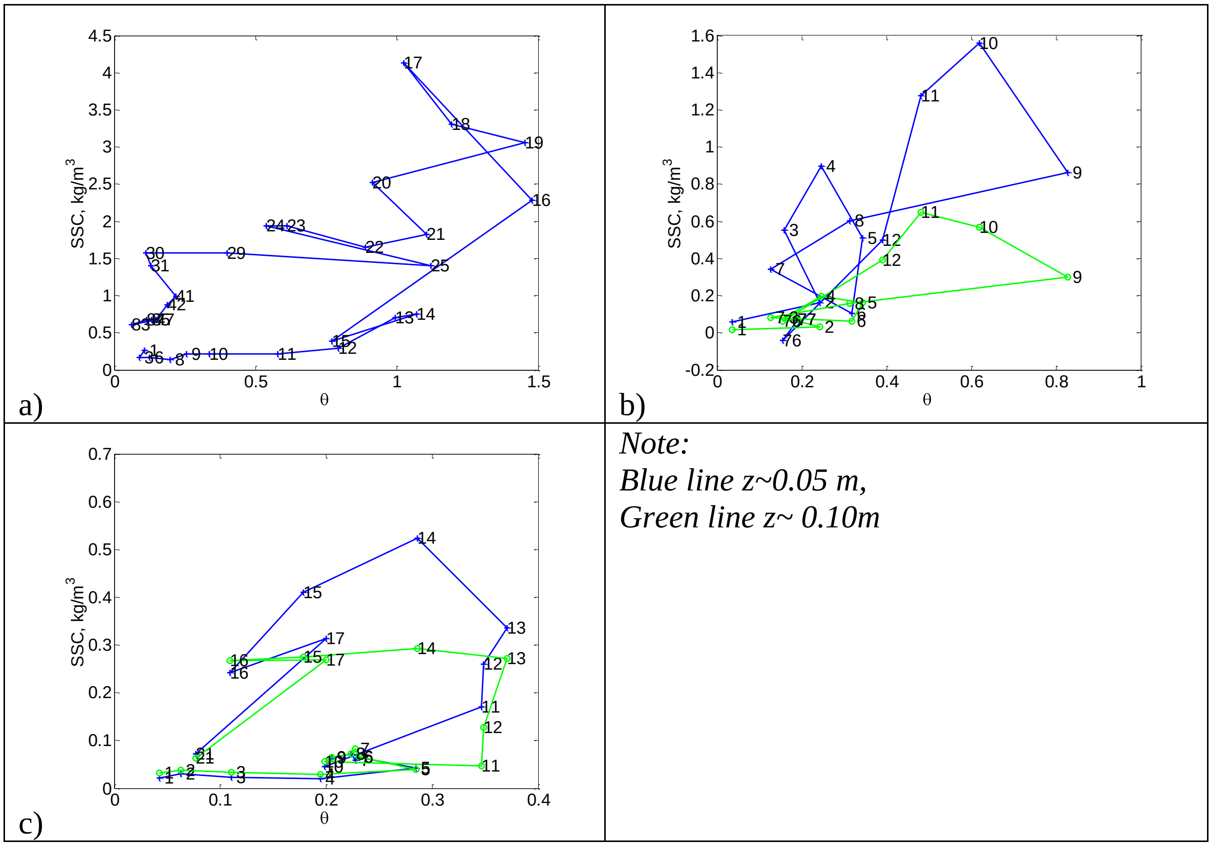

Figure 6. Phase diagrams of wave-by-wave θ'_w and *ssc* during high speed super-critical wakes: a) Torpedo Bay, Auckland, *QuickCat*; b) Tin Shed Bar, Snake River, *Hells Canyon Dream*; c) Salt Creek Bar, Snake River, *Happy Hour*

The LSV model was calibrated for two powerboats, a 26-ft workboat and a 44-ft tour boat, using wake data collected at Fish Trap Bar on the Snake River (Figures 7 and 8). A wave climate for the site was constructed from the number of boat passes measured and by running the LSV model a total of four times at each site (2 boats × 2 directions). Data manipulation programs were used to convert the LSV data into individual standard wave time series files. A wake time series for the 48-hour period was constructed by distributing the appropriate number of wake events, between the hours of 06:00 and 18:00 of each day. The periods between were taken as river-only periods.

A flow time series file for Fish Trap Bar was developed in an analogous manner to that of wake climate. Recorded discharges were used to estimate local discharges at the sand bar site. Instantaneous hourly flows were interpolated from steady-state MIKE 21C results (5,000 cfs, 10,000 cfs, 20,000 cfs, 30,000 cfs, 50,000 cfs, 75,000 cfs, and 100,000 cfs). The discharge hydrograph for the Fish Trap bar site from 8-27-2005 to 8-29-2005 is shown in Figure 9; time is represented in hours since start of the simulation. Also shown in Figure 9 are the periods of boating activity.

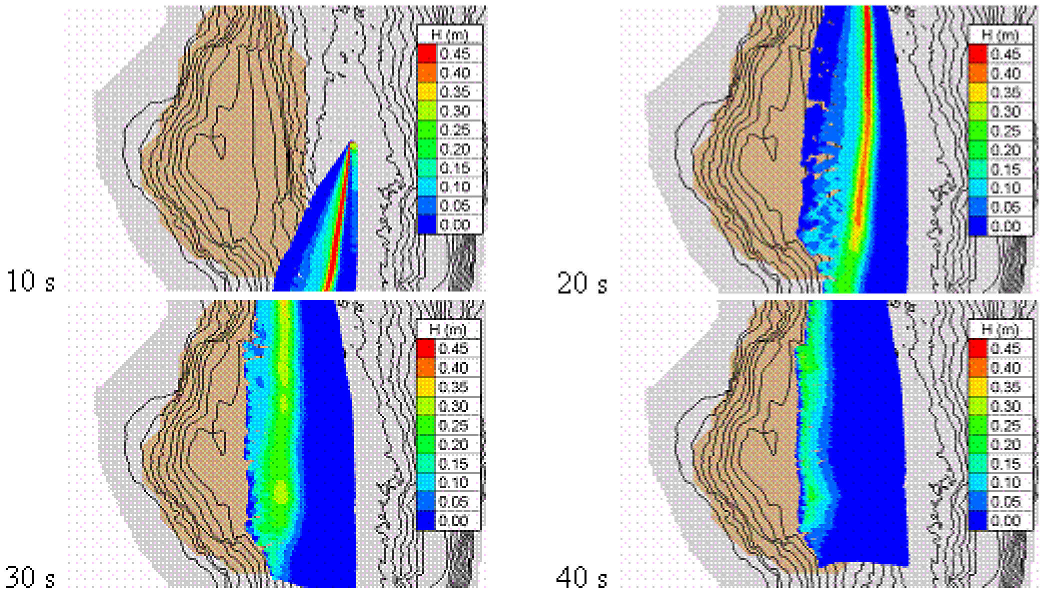

Figure 7. Time sequence of wake height at Fish Trap Bar on the Snake River produced by a 44-ft tour boat at 25 knots headed downstream

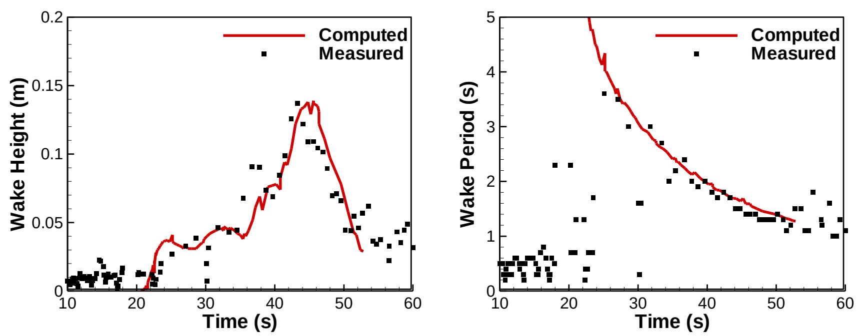

Figure 8. Comparison of measured and computed wake height (left) and period (right) for a 26.ft workboat headed downstream at Fish Trap Bar

The potential sediment transport rate predicted by the Camenen and Larson total load sediment transport formula was calibrated using optical backscatter *ssc* data collected at the study site. The calibration procedure involved operating PTM for a single boat passage and computing the instantaneous sediment load (i.e. the mass of sediment in the water column per unit area). Calibration of the model was obtained by adjusting the value of k_d in the Camenen and Larson formula until the measured and computed values of the sediment load in the water column agreed. A value of k_d =0.015 was found to provide the best calibration. This value falls within the range of values suggested by Camenen and Larson.

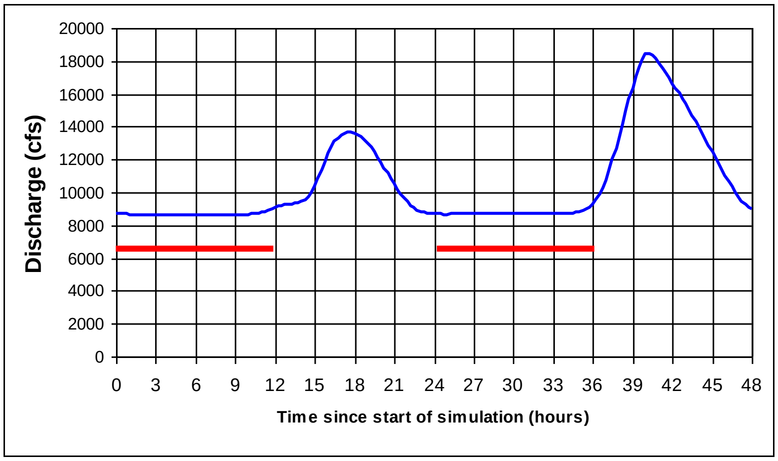

Figure 9. Discharge hydrograph at Fish Trap Bar over 48 hour simulation period. Red bars indicate periods of boating activity

In order to compare the measured results with the computed, they must first be time-averaged and depth-integrated. A two-second time-averaging window was used. Depth integration was performed using an assumed two-part concentration distribution. The concentration was assumed to be uniform over the lower 4 cm and to vary in a parabolic fashion above that point to the surface. Using this distribution a time series of the total suspended sediment load, M is computed (expressed in kg/m^2). Figure 10 shows the generally good agreement obtained between the estimated mass load of sediment in suspension based on field measurements at the study site and that predicted from the preliminary PTM run. The model tends to overpredict the suspended load in the early part of the wake and underpredict it later in the wake; this reflects the "wave group-induced" hysteresis observed in the measurements which is not accounted for in the sediment transport formula (Figure 6).

The results of the PTM simulation for the 48-hour period are presented in Figure 11. A general pattern of movement was observed in the results:

- boat wakes caused bed material to be brought into suspension;
- while in suspension, the ambient river currents and small wake-induced undertow caused a small, but important advection of the suspended material;
- the alongshore and offshore directed advection caused by multiple boat passages (35 on the first day and 23 on the second) and the river flow moved the material into deeper water, and;
- the larger discharge during the evening hours transported the material away from the site. This can be observed in the results at hours 18 and 39.

The general pattern of movement described above was observed at each of the sand bar sites studied on the Snake River. The river flows alone are not sufficient to mobilize sand sized material in the nearshore zone. Boat wakes do put material into suspension. While in suspension, river flows and the wake-induced undertow gradually move the material along and across the nearshore zone. Often the material was moved into deeper water, where it was later removed when larger flows occurred.

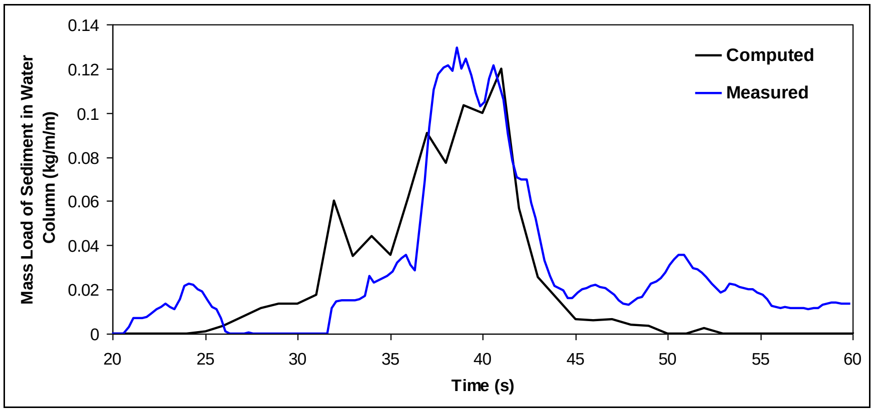

Figure 10. Comparison of measured and computed sediment load in the water column per unit bed area

CONCLUSION

Analysis of a large number of velocity records from several sites reveals that as well as introducing an oscillatory component to the nearshore current, the boat wakes also modify the local steady current by producing an offshore-directed flow. The offshore-directed flow has not been previously documented in the context of vessel wakes though it appears to be analogous to a group-forced second-order flow and set-up driven undertow. A relatively simple undertow model Grasmeijer and Ruessink (2003) is found to be in good agreement with the measured flow.

Suspended load and bedload modes appear to respond differently to waves of varying frequency in a super-critical wake group sequence. Osborne et al. (in press) describe how the longer period motions at the start of a super-critical boat wake result in net offshore transport of gravel and cobble on mixed beaches in Puget Sound. In this paper, the time varying suspension patterns under super-critical wakes are shown to exhibit properties similar to the suspension patterns under conventional wave groups produced by ocean waves (e.g. Villard et al., 2000). The *ssc* remains elevated for a number of waves following the peak velocities under the higher frequency waves in a wake group resulting in a hysteresis between the maximum wave component of bed shear stress and the ssc.

Model simulations combining the hydrodynamics of super-critical wakes with steady currents and a sand transport model provide results that are consistent with the field measurements and observations of the suspended load fraction. The wakes re-suspend sand in the nearshore that would otherwise be immobile. The sand is transported both alongshore and offshore incrementally away from the shoreline eventually reaching deeper water where stronger ambient flows can transport the sediment.

Although the model incorporates some of the elements of the wake induced mean flows, the approach does not fully account for the wave group-induced hysteresis on the suspended sediment load or the differential effects of wave frequency and shape (nonlinearity) effects on the suspended load and bedload. More work is also needed to model the tendency for offshore transport of sand, gravel, and cobble-sized sediment on mixed sediment beaches under super-critical wakes, that leads to beach flattening, while their sub-critical counterparts often lead to beach steepening.

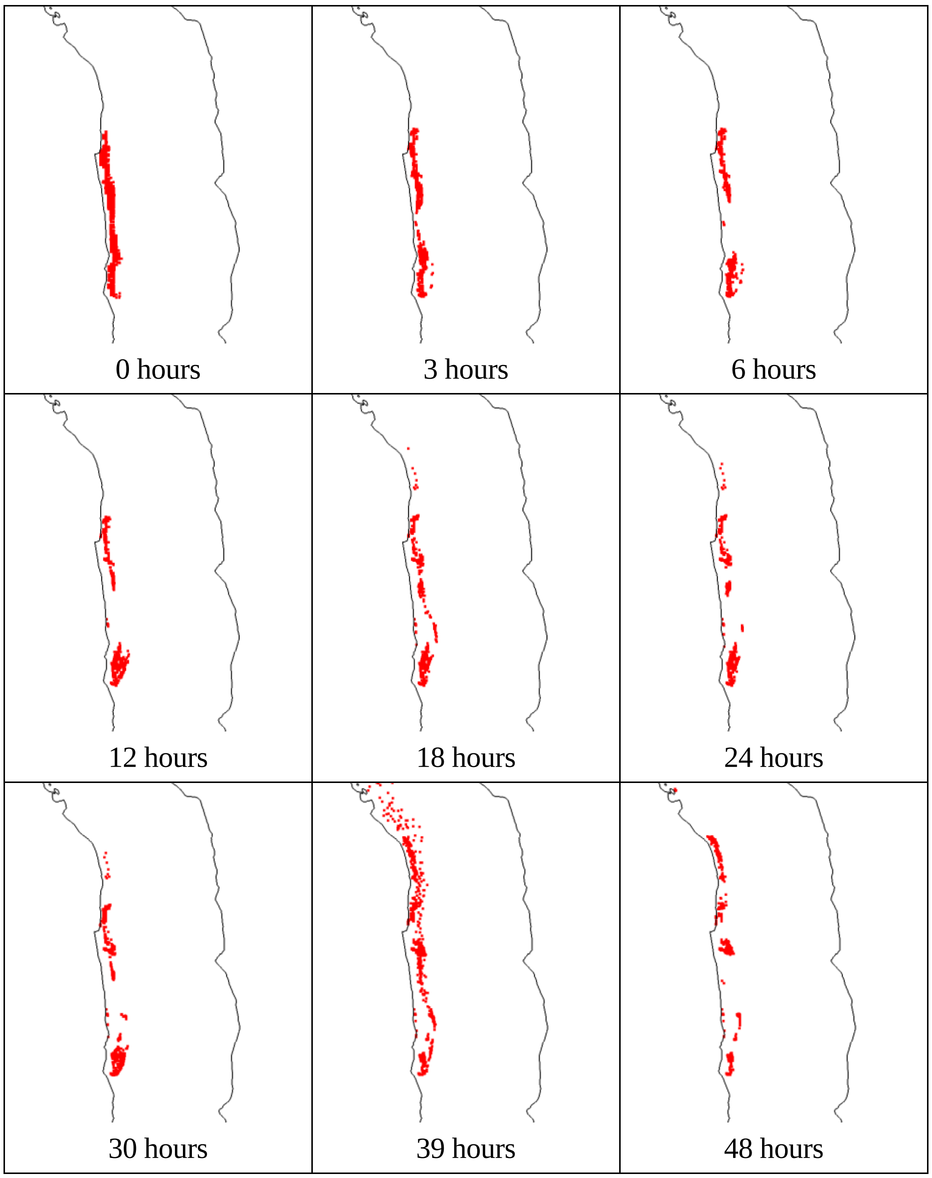

Figure 11. PTM model results for the river plus wake simulation at Fish Trap Bar

ACKNOWLEDGEMENTS

This work would not have been possible without the cooperation and assistance of many people: past and present PI Engineering staff assisted with data collection and processing; the waterfront property owners of Rich Passage continue to provide access to beaches, and the vessel operators have provided the wakes and vessel performance information. Their contributions are gratefully acknowledged. The development of LSV was funded by a federal grant program administered by the Federal Transportation Administration (FTA-WA-26-7007-2005), designed to support research and investigations of emerging transportation systems. Idaho Power Company (IPC) funded the studies on the Snake River; IPC staff also assisted with data collection and kindly granted permission to publish the results.

REFERENCES

Camenen, B. and Larson, M. (in press) "General sediment transport formula for waves and current." Coastal Engineering (submitted 2006).

Doering, J.R.C. (1988) Wave-wave interactions in the nearshore. Ph.D thesis, Department of Oceanography, Dalhousie University, Halifax, NS, 139p.

Grasmeijer, B.T. and Ruessink, B.G. (2003). Modeling of waves and currents in the nearshore parametric vs. probabilistic approach. Coastal Engineering, 49: 185-207.

Longuet-Higgins, M.S. and Stewart, R.W. (1962) Radiation stress and mass transport in gravity waves, with application to surf-beats. Journal of Fluid Mechanics, 13: 481-504.

Longuet-Higgins, M.S. and Stewart, R.W. (1964) Radiation stress in water waves: a physical discussion with applications. Deep Sea Research, 11: 529-562.

MacDonald, N.J., 2005. Super-Critical Vessel Modeling. In: Proceedings, Canadian Coastal Conference 2005, Halifax, on CDROM.

MacDonald, N. J., M. H. Davies, A. Z. Zundel, J. D. Howlett, Z. Demirbilek, J. Z. Gailani, T. C. Lackey, and S. J. Smith. 2006. PTM: Particle tracking model, report 1: model theory, implementation, and example applications. Technical Report ERDC/CHL TR-06-20. Vicksburg, MS: U.S. Army Engineer Waterways Experiment Station, Hydraulics Laboratory.

Osborne, P.D. MacDonald, N.J. and Reynolds, W.J. (in press) Response of mixed sediment beaches to wake wash from passenger only fast ferries: Rich Passage, Washington. Proc. 30th International Conference on Coastal Engineering, San Diego, CA, ASCE, Sept 2006.

Parnell KE and Kofoed-Hansen H. 2001. Wakes from large high-speed ferries in confined coastal waters: Management approaches with examples from New Zealand and Denmark, Coastal Management 29(3), 217-237

Villard, P.V., P.D. Osborne, C.E. Vincent. 2000. Influence of wave groups on SSC patterns over vortex ripples. Continental Shelf Research. 20 (17): 2391-2410.